Synthesis and Catalytic Properties of Au–Pd Nanoflowers

Jianguang Xu,[†,‡] Adria R. Wilson,[†] Aaron R. Rathmell,[†] Jane Howe,[§] Miaofang Chi,[§] and Benjamin J. Wiley[†,*]

[†]Department of Chemistry, Duke University, 124 Science Drive, Box 90354, Durham North Carolina 27708, United States, [‡]School of Electromechanical Engineering, Hunan University of Science and Technology, Xiangtan, Hunan 411201, China, and [§]Microscopy Group, Oak Ridge National Laboratory, 1 Bethel Valley Road, Building 4515, MS 6064, Oak Ridge, Tennessee 37831, United States

ABSTRACT Reduction of Pd ions by hydroquinone in the presence of gold nanoparticles and polyvinylpyrrolidone resulted in the formation of nanoflowers with a Au core and Pd petals. Addition of HCl to the synthesis halted the reduction by hydroquinone and enabled the acquisition of snapshots of the nanoflowers at different stages of growth. TEM images of the reaction after 10 s show that the nanoflower morphology resulted from the homogeneous nucleation of Pd clusters in solution and their subsequent attachment to gold seeds coated with a thin (0.8 ± 0.1 nm) shell of Pd. UV–visible spectra also indicate Pd clusters formed in the early stages of the reaction and disappeared as the nanoflowers grew. The speed at which this reaction can be halted is useful not only for producing a variety of bimetallic nanostructures with precisely controlled dimensions and morphologies but also for understanding the growth mechanism of these structures. The ability of the AuPd core–shell structure to catalyze the Suzuki coupling reaction of iodobenzene to phenylboronic acid was probed and compared against the activity of Pd nanocubes and thin-shelled AuPd core–shell nanoparticles. The results of this study suggest that Suzuki coupling was not affected by the surface structure or subsurface composition of the nanoparticles, but instead was primarily catalyzed by molecular Pd species that leached from the nanostructures.

KEYWORDS: gold · palladium · nanostructures · nanoflowers · nanoclusters

Au–Pd nanoparticles are excellent catalysts for a number of reactions, including the production of vinyl acetate,[1] the oxidation of primary alcohols to aldehydes,[2,3] the hydrochlorination of acetylene,[4,5] and the direct synthesis of H_2O_2 from H_2 and O_2.[6] The cooperative catalytic properties of Au and Pd exhibit the most dramatic effect in the oxidation of primary alcohols. For example, the oxidation of benzyl alcohol to benzaldehyde can be accelerated by 10 to 100 times through the use of Au_{core}–Pd_{shell} (Au_cPd_s) nanoparticles in place of Pd or Au nanoparticles, respectively.[2] The origins of this powerful cooperative effect, as well as the reaction mechanism, are not known. One reason for this lack of understanding is that the methods normally used to produce these catalysts (*e.g.*, impregnation, co-precipitation) result in nanoparticles with an ambiguous structure and composition, making it difficult to correlate properties and performance.

Recognizing the need for better control, researchers have begun to use colloidal synthesis to tune the size, shape, and composition of nanoparticle catalysts. These syntheses generally fall into two categories: (1) co-reduction, in which ions of both metals are reduced simultaneously, and (2) seeded synthesis, in which one starts with a seed nanoparticle of one composition and grows a shell around it. In the case of nanoparticles containing Au and Pd, a variety of syntheses that use either co-reduction[7–10] or a seeded approach have been reported.[11–14] In general, the seeded approach enables greater control over the shell thickness and morphology of the nanoparticle product. In one example, researchers have reduced H_2PdCl_4 with ascorbic acid to grow Pd shells on gold nanoparticles with thicknesses ranging from 11.5 to 44 nm.[11] Bimetallic Au_cPd_s nanocubes have been made by growing Pd onto Au octahedra.[12] Particles with a raspberry-like morphology have been obtained by growing Pd on hollow gold shells.[13]

We report a simple reaction scheme that utilizes hydroquinone as the reducing agent to grow Pd shells on Au seeds. Addition of a small amount of HCl effectively quenches the reducing power of hydroquinone and halts the reaction. This reaction scheme not only allows precise control over the thickness and morphology of the Pd shell but further enables the acquisition of snapshots of the growth process that provide insight into the mechanism by which nanoflowers form.

Methods for precisely tuning the morphology of nanostructures are valuable in that they can be used to generate specific structures for probing the structure–function relationships of heterogeneous nanoparticle catalysts. For example, the mechanism by which palladium nanoparticles catalyze the Suzuki–Miyaura carbon–carbon coupling

* Address correspondence to benjamin.wiley@duke.edu.

Received for review October 18, 2010 and accepted July 1, 2011.

Published online July 15, 2011
10.1021/nn201161m

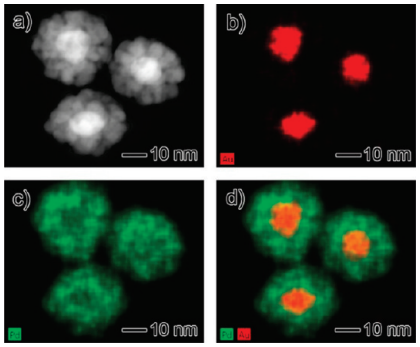

Figure 1. (a) HAADF-STEM image of nanoflowers consisting of a Au core and Pd petals. (b–d) Elemental maps obtained with EDX spectroscopy showing the distribution of Au and Pd in the nanoflowers.

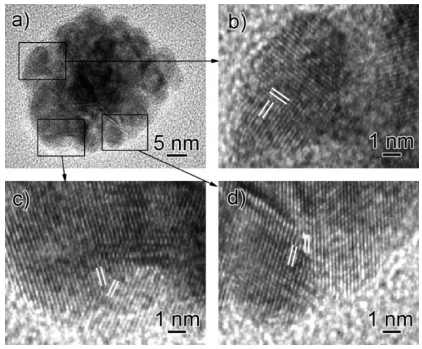

Figure 2. (a) HRTEM image of a nanoflower consisting of a Au core and Pd petals. (b–d) Higher magnification images illustrate the polycrystalline nature of the Pd shell. White lines indicate the direction of lattice fringes in different crystalline domains.

reaction remains somewhat ambiguous.[15] Leaching of Pd from the nanoparticles into solution is often observed during the reaction, and thus it is not entirely clear whether the Pd on the nanoparticle surface or Pd ions in solution act as the primary catalyst for the reaction.[15–21] To gain insight into how different AuPd nanostructures catalyze the Suzuki reaction, we have measured the rate of Suzuki coupling over Au_cPd_s nanoflowers, Pd nanocubes, and $Au_{core}–Pd_{thin\text{-}shell}$ (Au_cPd_{ts}) nanoparticles. Our experimental results indicate that the observed catalytic activity can be attributed to molecular Pd species that leached from the nanostructures over the course of the reaction. As nanostructures possessing lower (nanocubes) and higher (nanoflowers) densities of low-coordination surface atoms leached the same amount of Pd into solution, the rate of Suzuki coupling in the presence of these nanostructures proved to be insensitive to morphology.

RESULTS AND DISCUSSION

Synthesis of Au_cPd_s Nanoflowers. Au nanospheres with an average diameter of 14.0 ± 1.3 nm were synthesized by boiling 31.2 mL of an aqueous solution containing 0.25 mM $HAuCl_4$ and 0.03 wt % of $Na_3C_6H_5O_7$ over a period of 10 min.[22] The resultant Au seeds were washed with deionized water and redispersed in 10 mL of an aqueous solution containing 0.2 mM Na_2PdCl_4 and 0.1 wt % PVP (55 000 MW). After bringing this solution to 50 °C while stirring at 300 rpm, 0.1 mL of 0.03 M aqueous hydroquinone was added to reduce the Pd onto the gold seeds.

TEM Characterization of Nanoflowers. Figure 1a shows a representative high-angle annular dark-field scanning TEM (HAADF-STEM) image of the nanoflowers obtained after allowing the reaction to occur for 15 min at 50 °C, at which point the particles are 33.5 ± 1.5 nm in diameter. This image clearly shows the high-contrast Au core (due to its higher atomic number) and the Pd petals of the nanoflower. An XRD pattern taken of the nanoflowers (Figure S1) shows the relative ratio of the different atomic planes nearly matches the standard powder diffraction pattern for Pd (Table S1). We used energy dispersive X-ray (EDX) spectroscopy in a STEM to map the elemental composition of the particle (Figure 1, b–d). The fact that the size of the Au core in the nanoflower (14.0 ± 0.7 nm) is nearly identical to the size of the starting seed (14.0 ± 1.3 nm) indicates that significant alloying between the Au core and the Pd shell did not occur. A HRTEM image (Figure 2) of a Au_cPd_s nanoflower shows the Pd petals consist of different crystalline domains, each approximately 3 nm in diameter. In Figure 2, b–d, lines are drawn to highlight the different orientation of lattice fringes in each crystalline domain. The polycrystalline nature of the Pd shell suggests that it grew *via* addition of small particles or clusters rather than by atomic addition or Ostwald ripening.

Determination of the Nanoflower Growth Mechanism. In order to determine how the nanoflower formed, we stopped the reaction at different time points and characterized the product with UV–visible (UV–vis) spectroscopy and TEM. To obtain accurate representations of the reaction at precise times, it was necessary to stop metal ion reduction quickly and reliably. This was accomplished by adding 0.1 mL of 0.3 M aqueous HCl to the reaction solution. The addition of HCl quenches the ion reduction because the reduction rate of the univalent form of hydroquinone (HQ^-) is $>10^4$ times faster than for the nonionized form, and since hydroquinone is a weak acid, the univalent form is not prevalent at low pH.[23,24] To confirm the effectiveness of this method, HCl was added to a reaction after 1 min, and a UV–vis spectrum of the reaction solution was acquired both immediately after and 10 min after addition of HCl. Figure S2 shows there was no change in the spectra after addition of HCl, confirming that HCl effectively halted the reaction at that time point.

Figure 3 shows TEM images of the reaction product at specific time points. A very thin Pd shell (0.8 ± 0.1 nm)

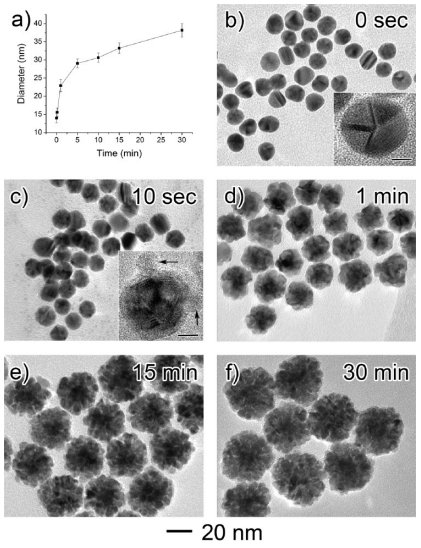

Figure 3. (a) Diameter of the Au_cPd_s nanoparticles *versus* time, as determined from TEM images. (b–f) TEM images of the nanoflower formation process, obtained by quenching the reaction with HCl at various time points. The inset of (c) shows clusters, indicated by arrows, attached to the Au_cPd_s nanoparticle. The scale bars in the insets are 5 nm.

was obtained after reducing Na_2PdCl_4 with hydroquinone for 10 s. The Pd shell grew very quickly during the first minute of the reaction, reaching a thickness of 4.5 ± 0.2 nm. The subsequent rate of growth decreased with time; the shell thickness increased by 5.3 ± 0.1 nm between 1 and 15 min and 2.3 ± 0.2 nm between 15 and 30 min. By 30 min, the conversion of Pd^{2+} into Pd^0 was 85.7%.

A higher magnification image of the 10 s time point (Figure 4a) provides another clue as to how the Au–Pd nanoflowers formed. This image shows that some of the Pd, instead of adding to the shell, homogeneously nucleated to form small clusters in the reaction solution. The inset of Figure 3c shows some of these clusters (indicated by arrows) adhered to the Au_cPd_s. The bumps (1 min) and branches (15 min) that appeared on the surface of the seed during the later stages of the reaction likely resulted from the addition of clusters to the seed.

UV–vis spectra of the reaction solution at different times further support our hypothesis that the nanoflowers grew *via* addition of clusters (Figure 4b). Initially, only the surface plasmon resonance (SPR) peak of the Au seed nanoparticles was present at 527 nm. This peak disappeared less than 10 s after adding hydroquinone to the reaction due to the formation of the thin Pd shell. At the same time, two new peaks appeared at 246 and 288 nm. The peak at 246 nm is associated with formation of metallic Pd. Our experimental evidence suggests that the peak at 288 nm is due to absorption by free Pd clusters in solution (it cannot be due to absorption by Pd^{2+}, as this species absorbs at 235 nm).[25] This assignment is supported by the fact that the intensity of the cluster peak decreases (and that of the Pd peak increases) after 5 min as branches form on the Pd shell due to addition of clusters (Figure 4c). The cluster peak disappeared completely at 30 min, after which no spectral change occurred. To provide further evidence for this peak assignment, we centrifuged the 10 s reaction solution at 5000 rpm for 10 min to separate the seeds from the clusters. Since the seeds are larger than the clusters, they are expected to form a pellet at the bottom of the tube, while the clusters remain in the supernate. As anticipated, the supernate exhibited the 288 nm peak associated with the clusters, while the resuspended pellet exhibited only the 246 nm peak associated with metallic Pd (Figure 4d). TEM images of the nanoparticles in the pellet also showed there were no Pd clusters present, but the clusters could be found in the TEM image of the supernate (insets of Figure 4d).

Role of Temperature and PVP in Nanoflower Formation. Both the reaction temperature and the presence of PVP play a critical role in the formation of nanoflowers. When the reaction temperature was increased to 100 °C, the Pd clusters grew too quickly and, rather than adding to the seed, formed larger Pd nanoparticles (Figure 5a). Without PVP, Pd clusters still added to the gold seeds, but many Pd clusters remained in solution after running the reaction for 15 min (Figure 5b), and the cluster peak at 288 nm failed to disappear. This result is somewhat counterintuitive in that PVP is usually added to a reaction solution to prevent aggregation of nanoparticles. In contrast, our findings suggest PVP somehow aids in the capture of the clusters by the seeds.

Cluster-mediated growth has recently been observed in the formation of Pt dendrites on a Pd core in the presence of PVP.[26] The authors noted that the observed attachment of Pt clusters to the Pd seed indicated that PVP was not effective at stabilizing the clusters against aggregation and coalescence. However, no control reactions were performed to determine if PVP *promoted* the capture of the Pt clusters by the Pd seed, *i.e.*, if the attachment occurred in the absence of PVP. In other work, PVP has been observed to promote the coalescence of Ag clusters into nanoparticles, and the final size of the particle has been observed to increase from 8 to 24 nm as the MW of the PVP increased from 10 000 to 1 300 000.[27] After the Ag particles reached a certain size, PVP stabilized the particles against aggregation. Taken together, these two previous papers and our own work suggest that PVP promotes agglomeration of clusters into particles of a certain size, after which it stabilizes them against further aggregation. At present, it is not entirely clear how PVP promotes agglomeration of clusters. Our current hypothesis for how PVP-induced agglomeration occurs is that the parts of the PVP polymer chain that are not bound to the surface of the seed act as hooks to capture free Pd clusters. In this way the

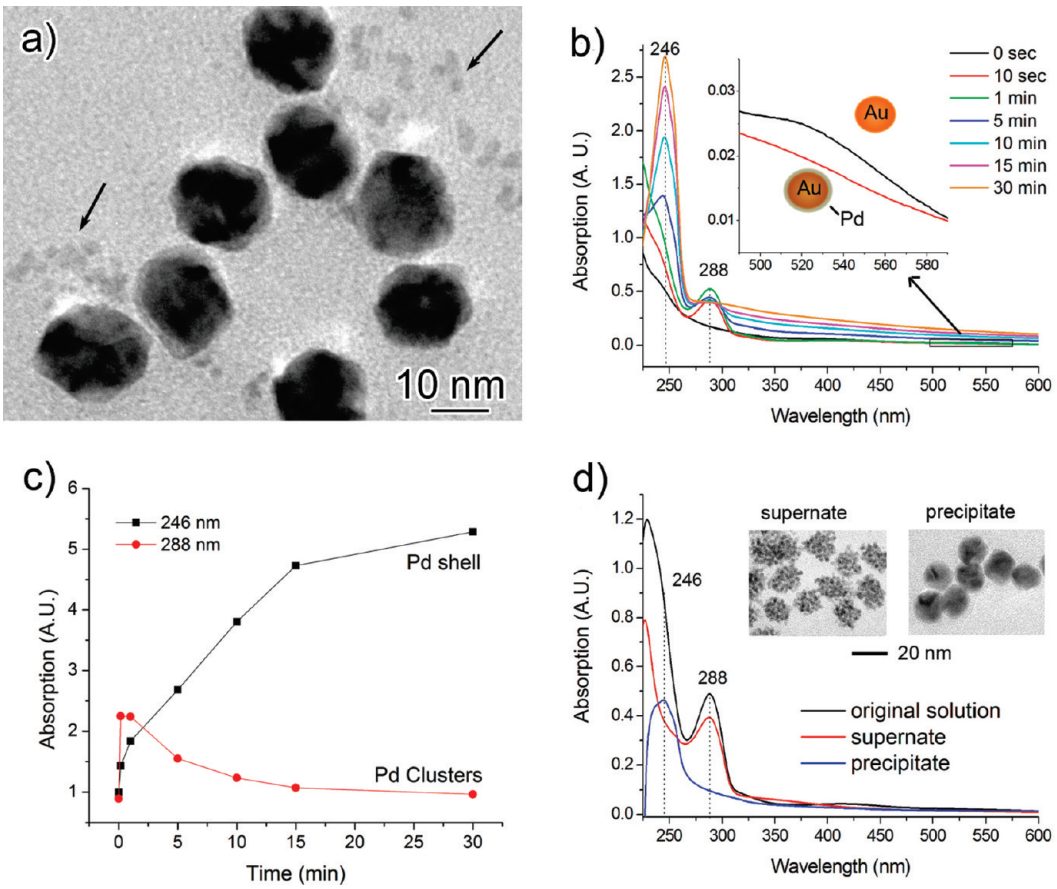

Figure 4. (a) Higher magnification TEM image of the reaction after 10 s shows the Pd clusters present in the reaction solution (indicated by arrows). (b) UV−vis spectra of the reaction solution at different reaction times. (c) Absorption of light by the Pd shell (246 nm) and Pd clusters (288 nm) *versus* time. The absorption at 246 nm has been normalized to the starting value. The absorption at 288 nm has been normalized to a baseline taken as the average of the intensity at 267 and 310 nm. (d) UV−vis spectra of the reaction solution at 10 s. This solution was centrifuged to separate clusters from particles. The spectrum of the supernate, which contained clusters (see inset TEM image), exhibited a peak at 288 nm. The spectrum of the precipitate, which contained particles but not clusters (see inset TEM image), did not exhibit the peak at 288 nm.

presence of PVP effectively increases the size of the seed, as well as its binding affinity for Pd clusters, and therefore increases the likelihood that the seed will collide with and capture Pd clusters. As a preliminary test for this hypothesis, we performed the reaction with PVP10 (MW = 10 000) instead of PVP55 (MW = 55 000), with the expectation that the shorter chain of PVP10 relative to PVP55 would result in a decreased ability to capture clusters. As expected, the rate of consumption of clusters in the presence of PVP10 was less than that for PVP55 (Figure 5e), suggesting that the relatively larger size of the PVP55 chain enhanced the capture of clusters by the seed.

Catalytic Activity of Nanoflowers for Suzuki Coupling. The activity of the Au_cPd_s nanoflowers for catalyzing the Suzuki coupling reaction between iodobenzene and phenylboronic acid was compared to the activities of the Pd nanocubes and the Au_cPd_{ts} nanoparticles. The synthesis of the Au_cPd_{ts} particles was carried out in the same manner as that of the Au_cPd_s nanoflowers, except that the ratio of Au to Pd was lowered from 1:20 to 2:1. The lower concentration of Pd in the thin-shell synthesis caused Pd to preferentially reduce onto the Au seeds as opposed to homogeneously nucleating and forming clusters. The Pd cubes are comprised of (100) surface facets and contain a relative low density of step and kink surface atoms compared to the smaller, highly curved clusters that make up the nanoflower. Thus, the nanocubes provide a control for determining whether the higher abundance of step and kink atoms improves the catalytic activity of the nanoflower.[28] The comparison with the Au_cPd_{ts} nanoparticles provides a control for the influence of the inner Au core on the catalytic behavior of Pd. The thickness of the Pd shell on the thin-shelled particles is 1.4 ± 0.1 nm, corresponding to a shell that is about five Pd atoms thick. At these dimensions, the potential electronic effects of Au on Pd may be more apparent than for the thick-shelled nanoflowers. The amount of nanoflowers added to catalyze the reaction was 0.25 mM on a Pd basis, which is the same amount used by Mohanty *et al.*[29] The amounts of Pd nanocubes and Au_cPd_{ts} nanoparticles added to the reaction were adjusted so that the surface area of the nanoparticles

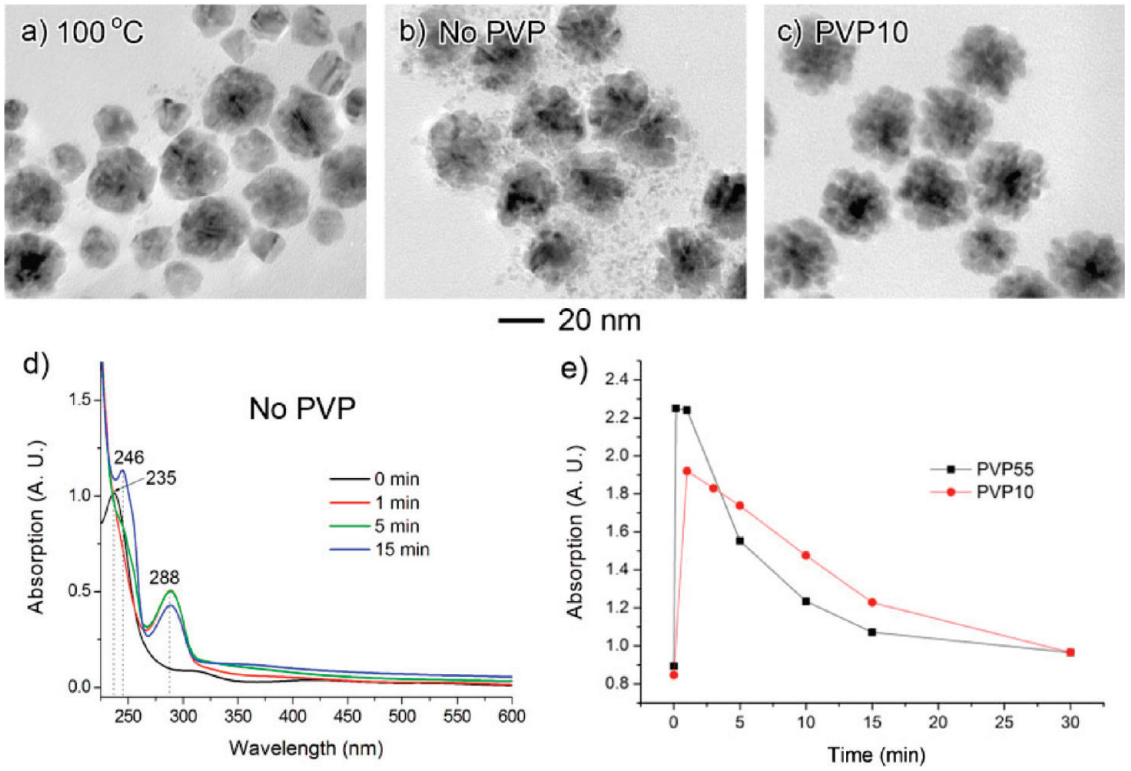

Figure 5. TEM images of Au_cPd_s nanoparticles obtained by running the reaction (a) at 100 °C (instead of 50 °C) for 15 min, (b) without PVP at 50 °C for 15 min, and (c) with PVP10 (MW = 10 000) at 50 °C for 15 min. (d) UV−vis spectra of the reaction in (b) show the cluster peak is prominent and does not disappear. The peak at 235 nm is due to absorption by Pd^{2+}, which is not visible in Figure 4 due to absorption by PVP.[20] (e) Comparison of absorbance at 288 nm *versus* time for the PVP10 and PVP55 reactions showing the clusters are more quickly consumed by the seeds in the presence of PVP55 than PVP10.

was the same for each reaction. Since it is not possible to assign a precise surface area to the nanoflowers due the unknown numbers of clusters attached to the surface and the level of consolidation between them, we approximated the surface area of the nanoflowers by measuring their diameter at their largest extent (from the edges of the outermost petals) and with this diameter calculated the surface area using the formula for a sphere. Although this is an approximate measure of the surface area of the nanoflowers, it should not underestimate the surface area by more than 50%.[30] TEM imaging was used to find the dimensions of the Pd nanocubes and Au_cPd_{ts} particles for the surface area calculation (Figure 6, c and d).

The Suzuki coupling of iodobenzene and phenylboronic acid resulted in the formation of biphenyl, which was isolated from the aqueous solution post-reaction along with any residual iodobenzene. Because iodobenzene is the limiting reagent in the reaction, the ratio of biphenyl to iodobenzene (as determined by NMR) provides the percent conversion to biphenyl. Conversion data gathered in this way (Figure 6a) revealed that there was no significant difference in the activity of any of the nanostructures. The fact that the conversion of the Au_cPd_s nanoflowers is no different from that of the Au_cPd_{ts} particles indicates that any effect of the Au core on the electronic structure of surface Pd atoms has no significant effect on the catalytic activity of the particle for Suzuki coupling. Additionally, the lack of a difference between the performance of the Pd nanocubes and the nanoflowers implies that the different arrangement of Pd atoms on the surface of these structures has no significant effect on the catalytic activity. This result is in contrast to recent work by Mohanty *et al.*, in which their results suggests the nanoflower has a greater activity than other morphologies for the Suzuki and Heck coupling reactions.[29] We note that these authors used other surfactants besides PVP for their nanostructure synthesis (sodium *N*-(4-*n*-dodecyloxybenzoyl)-L-isoleucinate) and that the use of PVP may have affected the catalytic performance of the nanoflowers or nanocubes. However, we note that Ellis *et al.* have previously observed structure-sensitive Suzuki coupling catalyzed by Pd nanoparticles synthesized in a 0.3 wt % solution of PVP.[31] We have used lower concentrations of PVP in the synthesis of Pd nanoflowers (0.1 wt %) and nanocubes (0.073 wt %). We have also washed the nanoparticles at least two times with DI water before the Suzuki coupling in an attempt to minimize the amount of PVP on the surface of the nanoparticles. Thus, given the previous results suggesting that PVP does not completely mask structure-sensitive effects in the Suzuki coupling reaction, we think it is unlikely that the

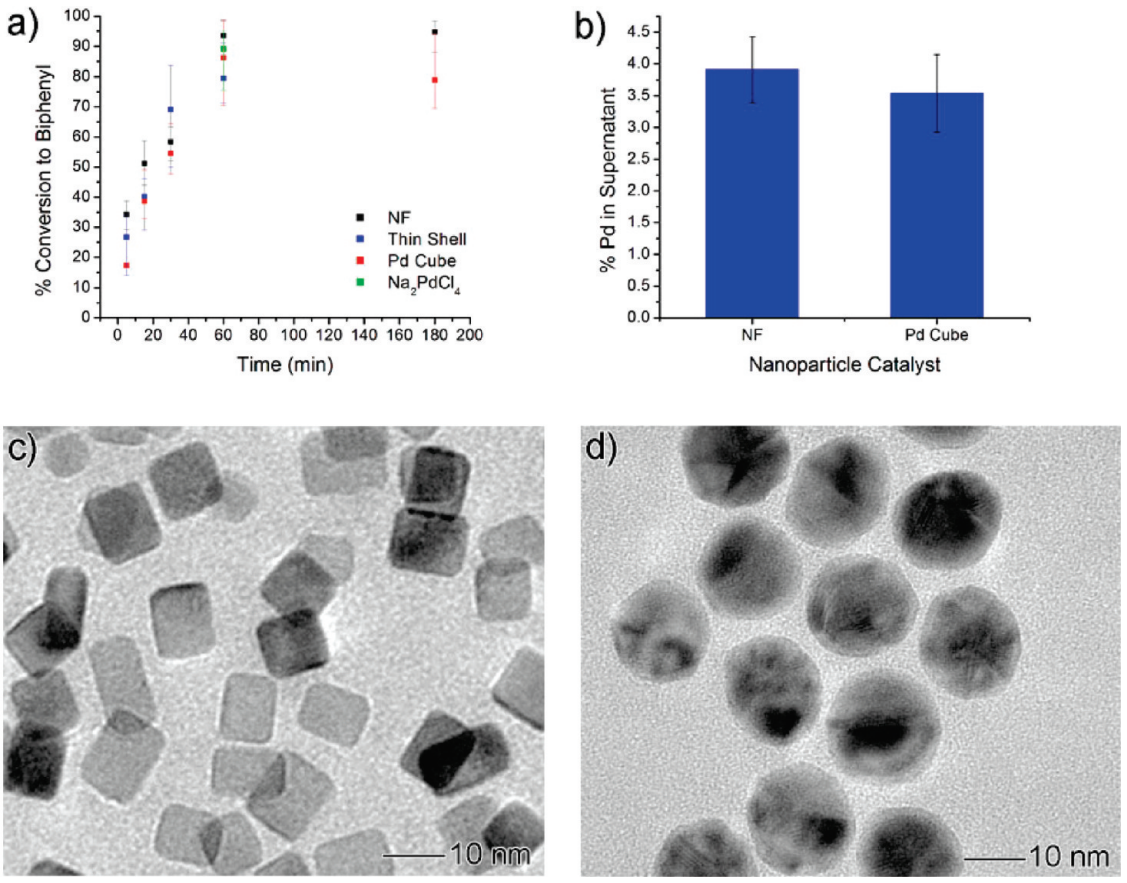

Figure 6. (a) Time-dependent catalytic activity of Au_cPd_s nanoflowers, Pd nanocubes, Au_cPd_{ts} nanoparticles, and Na_2PdCl_4 in the Suzuki coupling of iodobenzene and phenylboronic acid, expressed as percent conversion to biphenyl. (b) The percent of Pd ions that leached from the nanoparticles (expressed as a percent of the amount of Pd initially added to the reaction as nanoparticles) is indpendent of which type of particle was added. (c) TEM image of Pd nanocubes. (d) TEM image of Au_cPd_{ts} nanoparticles.

lack of structure-sensitivity in our results can be entirely attributed to the use of PVP.

We also note that if we underestimated the surface area of the nanoflowers (as may be the case), we would need to add more nanocubes or Au_cPd_{ts} particles to match the greater surface area of the nanoflowers. This would in turn make the nanoflowers appear less active than the other nanostructures. Thus we conclude that it is unlikely that any error in underestimating the surface area of nanoflowers can account for the fact that the nanoflower morphology is not more catalytically active than other morphologies.

There is an ongoing debate as to whether Suzuki coupling can be completely catalyzed heterogeneously (*i.e.*, on the surface of a Pd nanoparticle) or whether Suzuki coupling is always catalyzed by molecular Pd species.[15] Homogeneous Pd catalysts are thought to catalyze the Suzuki reaction by cycling between the Pd^0 and Pd^{2+} oxidation states, reaching the latter state by oxidative addition of the aryl halide to the Pd^0 complex.[16] The mechanism often put forth for how palladium nanoparticles catalyze carbon coupling is similar to the catalytic cycle for soluble Pd catalysts in that the reaction is catalyzed by molecular Pd species in solution, rather than on the surface of the nanoparticles.[17,18] It is believed that soluble Pd is leached from the surface of Pd nanoparticles through oxidative addition of the aryl halide.[18−21] Once the Pd in solution is returned to the zerovalent state after catalysis, it may remain in the catalytic cycle or redeposit on the nanoparticle surface. Hu and Liu studied the Suzuki coupling of bromobenzene to phenylboronic acid using polymer-stabilized Pd nanoparticles and observed a morphological transformation into needle-like structures after the catalyst was recycled several times. They attributed the morphological change to repeated dissolution and redeposition of Pd throughout the reaction and concluded that while Pd^0 may also exist in a discrete form on the polymer, Pd was primarily redeposited onto the original nanoparticles.[18] Cassol *et al.* and Reetz observed that Pd nanoparticles about 2 nm in diameter grew three times in size during a Heck coupling reaction through dissolution of and redeposition onto the original nanoparticles.[17,19] Additionally, Pd clusters have been found by de Vries and Reetz to precipitate as palladium black when the Pd concentration is sufficiently high and that this precipitation reduces the reaction rate.[19−21] These results support

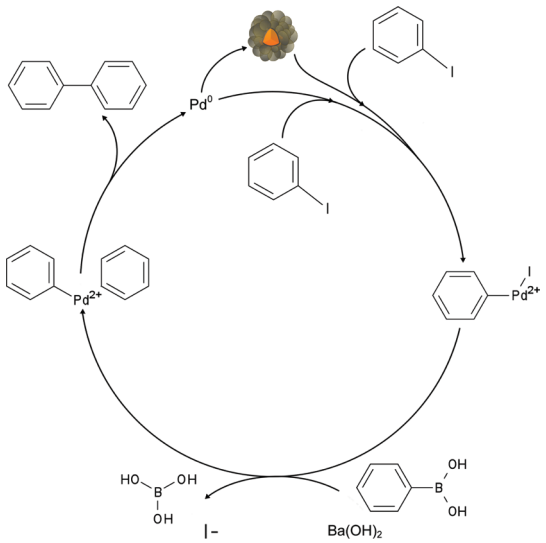

Figure 7. Reaction scheme for the Pd-catalyzed Suzuki coupling of iodobenzene to phenylboronic acid, adapted from several Suzuki coupling mechanisms.[14,24−29] Here, the source of Pd^0 is the surface of the Au_cPd_s nanoflower, shown in cross-section at the top of the scheme. Iodobenzene oxidizes Pd atoms on the nanoflower surface and introduces them into the catalytic cycle, which takes place in solution. Pd^{2+} is returned to Pd^0 *via* reductive elimination. Pd^0 can then either continue in the catalytic cycle or redeposit on the nanoparticle surface.

the hypothesis that nanoparticles act as a Pd reservoir and that the main catalytic cycle primarily depends upon soluble Pd species.

In order to determine if Pd had leached from the AuPd nanoflowers and nanocubes over the course of the Suzuki reaction, we performed atomic absorption spectroscopy (AAS) on the aqueous reaction phase after removing the nanoparticles by centrifugation. Figure 6b shows that after running the coupling reaction for 60 min the percentage of Pd dissolved in the supernate relative to the amount of Pd introduced to the reaction was roughly the same for both the nanoflowers (3.9 ± 0.5%) and the nanocubes (3.5 ± 0.6%). This result suggests that the similar activity of these nanostructures for Suzuki coupling could be due to the fact that a similar amount of Pd leached from their surface. To further test this hypothesis, we introduced Pd ions to the Suzuki coupling reaction in the form of Na_2PdCl_4 in an amount equal to the amount of Pd leached from the nanoflowers after 1 h, which was 0.087 mol % Pd relative to the initial iodobenzene concentration. After 1 h, the percent conversion of iodobenzene to biphenyl was determined to be 89.1 ± 9.2%. This value matches the conversions reported for the nanostructures in Figure 6a. This result further supports the hypothesis that molecular Pd species are the dominant catalyst in the Suzuki coupling reaction and that the nanoflowers and nanocubes primarily serve as a reservoir for Pd. Figure 7 schematically illustrates the current understanding of the reaction mechanism for the nanoparticle-catalyzed coupling of iodobenzene and phenylboronic acid.

CONCLUSIONS

We have shown that the morphology and shell thickness of Au_cPd_s nanoparticles can be tuned by quenching hydroquinone reduction with hydrochloric acid at precise time points. With a combination of UV−vis spectroscopy and TEM, we show that the high surface area, flower-like morphology resulted from the homogeneous nucleation of Pd clusters and their subsequent PVP-assisted addition to Au_cPd_s nanoparticles. Comparison of the catalytic activity of the Au_cPd_s nanoflowers against monometallic Pd nanocubes and Au_cPd_{ts} nanoparticles in the Suzuki coupling of iodobenzene to phenylboronic acid revealed that the conversion rate to biphenyl was not dependent upon the surface structure or subsurface composition of the particles. Instead, the observed catalytic activity for Suzuki coupling was attributed to molecular Pd species that leached from the Pd nanostructures. Given the ongoing debate and contradictory results regarding whether Suzuki coupling can be catalyzed heterogeneously, this reaction may be a less than ideal probe of the structure-sensitive catalytic properties of different nanostructure morphologies.

MATERIALS AND METHODS

Materials. Gold(III) chloride trihydrate (520918), sodium citrate tribasic dihydrate (S4641), sodium tetrachloropalladate(II) (205818), hydroquinone (H9003), polyvinylpyrrolidone MW = 55 000 (856568, PVP55), phenylboronic acid (78181), magnesium sulfate (63136), potassium bromide (221864), D-chloroform (151858), and L-ascorbic acid (A5960) were purchased from Sigma-Aldrich. Hydrochloric acid (UN1789), iodobenzene (122330050), barium hydroxide hydrate (377820050), and sodium chloride (M-11624) were purchased from Fisher Scientific. Methanol (BDH1135) and hexane (BDH1129) were purchased from VWR. All chemicals were used without further purification.

Reaction Preparation. Flasks and stir bars were cleaned with *aqua regia*, thoroughly rinsed with DI water, and dried in an 80 °C oven before use. Once dry, the flasks were allowed to cool to room temperature before any reactants were added.

Au Nanoparticle Seed Synthesis. A gold nanoparticle seed solution was prepared by sodium citrate reduction.[22] Briefly, 30 mL of DI water and 0.3 mL of 25 mM gold(III) chloride trihydrate were added to a 100 mL round-bottom flask. The solution was rapidly brought to a boil while stirring at 500 rpm, and 0.9 mL of 1 wt % sodium citrate tribasic dihydrate was added. The solution was removed from heat after 10 min.

Nanoflower Synthesis. Sodium tetrachloropalladate(II) solution was centrifuged at 15 000 rpm for 30 min in a microcentrifuge tube before use to remove any pre-existing clusters, after which volumes were pipetted off the top. To synthesize nanoflowers, 0.4 mL of as-prepared gold seed solution and 0.1 mL of 20 mM sodium tetrachloropalladate(II) solution were added

separately to 9.4 mL of DI water with 0.1 wt % PVP55. The mixture was put into a 50 mL round-bottom flask and heated to 50 °C, and 0.1 mL of 30 mM hydroquinone was added to the solution. To stop the reaction, 0.1 mL of 0.3 M HCl solution was added to the reaction, and the flask was cooled in ice water. For UV–vis measurements, the reaction solution was diluted 1:1 with DI water. For electron microscopy, the solutions were diluted 1:1 with methanol and centrifuged at 15 000 rpm for 10 min. The precipitates were washed again with a 1:1 mixture of methanol and water and dispersed in 0.2 mL of DI water.

Nanoflower Characterization. UV–vis absorption spectroscopy was performed on a Cary 6000i UV–vis–NIR spectrophotometer. Electron microscopy at Duke was performed with a FEI Tecnai G2 Twin TEM transmission electron microscope. High-resolution TEM was performed with a Hitachi HF-3300 FEG at Oak Ridge National Laboratory (ORNL). High-angle annular dark-field scanning TEM and energy-dispersive X-ray spectroscopy were performed on the JEOL 2200FS at ORNL. TEM images of the nanoflowers taken at the various time points were analyzed using ImageJ to obtain the dimensions of the nanoparticles (*e.g.*, outer diameters and shell thicknesses). The extent of Pd ion reduction onto the nanoflower surface was determined by AAS analysis of the reaction solution supernate after centrifugation to separate out the nanoflowers that had formed. XRD analysis was performed on a Panalytical X'Pert PRO MRD HR X-ray Diffraction System at Duke University.

Suzuki Coupling Reaction. The Suzuki coupling reaction procedure was adopted from the procedure used by Mohanty *et al.*[29] A 50 mL round-bottom flask was heated to 80 °C under reflux and with a spin rate of 450 rpm. The reaction solution contained enough water to make the total reaction volume 20 mL after the addition of the nanoparticle catalyst solution. The nanoflower synthesis was allowed to progress for 15 min. Pd nanocubes and thin-shelled AuPd nanoparticles were prepared as described below. All nanoparticles were washed by centrifugation and DI water at least two times and redispersed in DI water before addition to the coupling reaction. To the flask were added 0.1136 g of barium hydroxide dihydrate and 0.0536 g of phenylboronic acid. After waiting 5 min to allow for dissolution of the phenylboronic acid, 25 uL of iodobenzene was pipetted into the solution, immediately followed by the addition of the appropriate nanoparticle catalyst solution.

For testing in the Suzuki reaction, the Au_cPd_s nanoflower synthesis as described above was halted at 15 min and diluted with methanol to a volume ratio of 4:1 DI water:methanol. This solution was centrifuged at 15 000 rpm for 9 min, and the precipitate was then redispersed in DI water to its original volume. Enough of the 15 min nanoflower solution was used in the reaction for the Pd concentration to be 0.25 mM in the final reaction volume, but the volumes of the other two catalysts were determined by setting the surface area equivalent to that of the 15 min nanoflowers. The volume of nanoflower solution added to the reaction contained 2.41×10^{12} nanoflowers; the surface area of a single nanoflower was calculated to be 3525.65 nm^2, and thus the total surface area of the nanoflowers added to the reaction was 8.496×10^{15} nm^2. To match this, 1.755×10^{13} Pd nanocubes were added for each reaction, corresponding to a Pd concentration of 0.0775 mM in the final reaction solution. Similarly, 1.201×10^{13} thin-shelled AuPd nanoparticles were required to introduce the same surface area to the reaction, which corresponded to a Pd concentration of 0.0324 mM in the reaction solution. The concentrations of each nanoparticle solution were experimentally determined by AAS.

After the reaction, biphenyl and any other remaining iodobenzene were removed from the aqueous phase by extracting three times with 20 mL of hexane. The hexane layer was washed once with a saturated aqueous sodium chloride solution and was then dried by pouring it over just enough magnesium sulfate to form a slurry. The slurry was filtered gravimetrically, the residue was washed once with boiling hexane, the hexane was evaporated in a rotoevaporator, and the leftover organic was redissolved in a minimal amount of *d*-chloroform. The sample was tested immediately using NMR spectroscopy.

Characterization of Suzuki Reaction Products. Iodobenzene and biphenyl are soluble in hexane, while phenylboronic acid remains in the aqueous layer during the extraction step described above. Thus, the NMR sample contains only the limiting reagent iodobenzene and any biphenyl product formed. The relative intensities of peaks characteristic of either of the two compounds were normalized to the intensity per hydrogen, and the percentage conversion to biphenyl was calculated from the ratio of the two resultant peak intensities. The aqueous layer, which contains the nanoparticles and any solubilized Pd ion, was centrifuged once to remove the solid precipitate from the supernate. The supernate was centrifuged a second time to remove any remaining particulate Pd, but no additional precipitate was observed after the second centrifugation step. The supernate and precipitate samples were dissolved in 15% (v/v) *aqua regia*, and the relative amount of palladium in each was determined by AAS. The wavelength of analysis used was 340.6 nm.

Palladium Nanocube Synthesis. Pd nanocubes were made using the synthesis developed by Lim *et al.*[28] First, 0.0512 g of sodium tetrachloropalladate(II), 0.0966 g of PVP55, 0.2737 g of potassium bromide, and 0.0546 g of L-ascorbic acid were dissolved in 10 mL of DI water. This solution was then heated at 80 °C for 3 h while stirring at 400 rpm. After the reaction, the solution was diluted 10 times in DI water and centrifuged at 15 000 rpm for 10 min. The supernate was removed and centrifuged again under the same conditions; this process was repeated at least three times. The final volume of precipitated Pd cubes was rediluted with DI water, and the Pd concentration was determined using AAS.

Thin-Shelled Gold–Palladium Nanoparticle Synthesis. Following their synthesis as described above, 640 mL of the Au nanoparticles was cleaned by centrifugation for 1 h at a spin rate of 15 000 rpm in the presence of 0.03% (w/v) PVP55 and was subsequently resuspended in 380 mL of DI water. This solution was added to a 500 mL round-bottom flask with 10 mL of 1% PVP and 4 mL of 20 mM sodium tetrachloropalladate(II), and the mixture was heated to 50 °C while stirring at 400 rpm. Once the reaction reached 50 °C, which took about 20 min, 4 mL of 1% (w/v) hydroquinone was added to initiate the reduction of Pd onto the Au nanoparticle surface. The reaction was allowed to proceed for two hours before being stopped through the addition of 4 mL of 1% (v/v) hydrochloric acid solution. The nanoparticles were diluted with a 10% aqueous solution of methanol, centrifuged for 20 min at 15 000 rpm, and resuspended in DI water. The main difference between the synthesis of nanoflowers and thin-shelled particles was the relative amount of Pd introduced to the reaction. In the nanoflower synthesis, the Au:Pd ratio was 1:20; in the thin-shell synthesis the Au:Pd ratio was 1:0.5. The reaction time also differed substantially. The nanoflowers used in Suzuki coupling were those formed after 15 minutes of reaction, whereas the Au_cPd_{ts} nanoparticles reacted for two hours.

Acknowledgment. This research was supported by start-up funds from Duke University, the China Scholarship Council (fellowship to J.X.), and ORNL's Share User Facility (J.H. and M. C.), which is sponsored by the Scientific User Facilities Division, Office of Basic Energy Sciences, U.S. Department of Energy. A.R. W. acknowledges support by a fellowship from the Graduate Certificate Program in Nanoscience at Duke University.

Supporting Information Available: Figures S1, S2 and Table S1. This material is available free of charge *via* the Internet at http://pubs.acs.org.

REFERENCES AND NOTES

1. Thompson, D. T. Catalysis by Gold/Platinum Group Metals. *Platinum Met. Rev.* **2004**, *48*, 169–172.
2. Enache, D. I.; Edwards, J. K.; Landon, P.; Solsona-Espriu, B.; Carley, A. F.; Herzing, A. A.; Watanabe, M.; Kiely, C. J.; Knight, D. W.; Hutchings, G. J. Solvent-Free Oxidation of Primary Alcohols to Aldehydes using Au-Pd/TiO_2 Catalysts. *Science* **2006**, *311*, 362–365.
3. Marx, S.; Baiker, A. Beneficial Interaction of Gold and Palladium in Bimetallic Catalysts for the Selective Oxidation of Benzyl Alcohol. *J. Phys. Chem. C* **2009**, *113*, 6191–6201.

4. Lee, A. F.; Baddeley, C. J.; Hardacre, C.; Ormerod, R. M.; Lambert, R. M.; Schmid, G.; West, H. Structural and Catalytic Properties of Novel Au/Pd Bimetallic Colloid Particles: EXAFS, XRD, and Acetylene Coupling. *J. Phys. Chem.* **1995**, *99*, 6096–6102.
5. Conte, M.; Carley, A. F.; Attard, G.; Herzing, A. A.; Kiely, C. J.; Hutchings, G. J. Hydrochlorination of Acetylene Using Supported Bimetallic Au-Based Catalysts. *J. Catal.* **2008**, *257*, 190–198.
6. Piccinini, M.; Ntainjua, E.; Edwards, J. K.; Carley, A. F.; Moulijn, J. A.; Hutchings, G. J. Effect of the Reaction Conditions on the Performance of Au-Pd/TiO_2 Catalyst for the Direct Synthesis of Hydrogen Peroxide. *Phys. Chem. Chem. Phys.* **2010**, *12*, 2488–2492.
7. Liu, F.; Wechsler, D.; Zhang, P. Alloy-Structure-Dependent Electronic Behavior and Surface Properties of Au-Pd Nanoparticles. *Chem. Phys. Lett.* **2008**, *461*, 254–259.
8. Wu, M.-L.; Chen, D.-H.; Huang, T.-C. Synthesis of Au/Pd Bimetallic Nanoparticles in Reverse Micelles. *Langmuir* **2001**, *17*, 3877–3883.
9. Harpeness, R.; Gedanken, A. Microwave Synthesis of Core-Shell Gold/Palladium Bimetallic Nanoparticles. *Langmuir* **2004**, *20*, 3431–3434.
10. Lee, Y. W.; Kim, M.; Kim, Z. H.; Han, S. W. One-Step Synthesis of Au@Pd Core-Shell Nanooctahedron. *J. Am. Chem. Soc.* **2009**, *131*, 17036–17037.
11. Hu, J.-W.; Zhang, Y.; Li, J.-F.; Liu, Z.; Ren, B.; Sun, S.-G.; Tian, Z.-Q.; Lian, T. Synthesis of Au@Pd Core-Shell Nanoparticles with Controllable Size and Their Application in Surface-Enhanced Raman Spectroscopy. *Chem. Phys. Lett.* **2005**, *408*, 354–359.
12. Fan, F.-R.; Liu, D.-Y.; Wu, Y.-F.; Duan, S.; Xie, Z.-X.; Jiang, Z.-Y.; Tian, Z.-Q. Epitaxial Growth of Heterogeneous Metal Nanocrystals: From Gold Nano-octahedra to Palladium and Silver Nanocubes. *J. Am. Chem. Soc.* **2008**, *130*, 6949–6951.
13. Liu, Z.; Zhao, B.; Guo, C.; Sun, Y.; Xu, F.; Yang, H.; Li, Z. Novel Hybrid Electrocatalyst with Enhanced Performance in Alkaline Media: Hollow Au/Pd Core/Shell Nanostructures with a Raspberry Surface. *J. Phys. Chem. C* **2009**, *113*, 16766–16771.
14. Wang, F.; Li, C.; Sun, L.-D.; Wu, H.; Ming, T.; Wang, J.; Yu, J. C.; Yan, C.-H. Heteroepitaxial Growth of High-Index-Faceted Palladium Nanoshells and Their Catalytic Performance. *J. Am. Chem. Soc.* **2010**, *133*, 1106–1111.
15. Phan, N. T. S.; Van Der Sluys, M.; Jones, C. W. On the Nature of the Active Species in Palladium Catalyzed Mizoroki–Heck and Suzuki–Miyaura Couplings – Homogeneous or Heterogeneous Catalysis, A Critical Review. *Adv. Synth. Catal.* **2006**, *348*, 609–679.
16. Suzuki, A. Recent Advances in the Cross-Coupling Reactions of Organoboron Derivatives with Organic Electrophiles, 1995–1998. *J. Org. Chem.* **1999**, *576*, 147–168.
17. Cassol, C. C.; Umpierre, A. P.; Machado, G.; Wolke, S. I.; Dupont, J. The Role of Pd Nanoparticles in Ionic Liquid in the Heck Reaction. *J. Am. Chem. Soc.* **2005**, *127*, 3298–3299.
18. Hu, J.; Liu, Y. Pd Nanoparticle Aging and Its Implications in the Suzuki Cross-Coupling Reaction. *Langmuir* **2005**, *21*, 2121–2123.
19. Reetz, M. T.; de Vries, J. G. Ligand-Free Heck Reactions using Low Pd-Loading. *Chem. Commun.* **2004**, 1559–1563.
20. de Vries, A. H. M.; Mulders, J. M. C. A.; Mommers, J. H. M.; Henderickx, H. J. W.; de Vries, J. G. Homeopathic Ligand-Free Palladium as a Catalyst in the Heck Reaction. A Comparison with a Palladacycle. *Org. Lett.* **2003**, *5*, 3285–3288.
21. de Vries, J. G. A Unifying Mechanism for All High-Temperature Heck Reactions. The Role of Palladium Colloids and Anionic Species. *Dalton Trans.* **2006**, 421–429.
22. Perrault, S. D.; Chan, W. C. W. Synthesis and Surface Modification of Highly Monodispersed, Spherical Gold Nanoparticles of 50–200 nm. *J. Am. Chem. Soc.* **2009**, *131*, 17042–17043.
23. James, T. H. The Reduction of Silver Ions by Hydroquinone. *J. Am. Chem. Soc.* **1939**, *61*, 648–652.
24. McAuley, A. S., L.; West, P. R. Kinetics and Mechanism of the Oxidation of Benzenediols and Ascorbic Acid by bis(1,4,7-triazacyciononane)nickel(III) in Aqueous Perchlorate Media. *Can. J. Chem.* **1985**, *63*, 1198–1203.
25. Teranishi, T.; Miyake, M. Size Control of Palladium Nanoparticles and Their Crystal Structures. *Chem. Mater.* **1998**, *10*, 594–600.
26. Lim, B.; Jiang, M.; Yu, T.; Camargo, P.; Xia, Y. Nucleation and Growth Mechanisms for Pd-Pt Bimetallic Nanodendrites and their Electrocatalytic Properties. *Nano Res.* **2010**, *3*, 69–80.
27. Shin, H. S.; Yang, H. J.; Kim, S. B.; Lee, M. S. Mechanism of Growth of Colloidal Silver Nanoparticles Stabilized by Polyvinyl Pyrrolidone in [Gamma]-Irradiated Silver Nitrate Solution. *J. Colloid Interface Sci.* **2004**, *274*, 89–94.
28. Lim, B.; Jiang, M.; Tao, J.; Camargo, P. H. C.; Zhu, Y.; Xia, Y. Shape-Controlled Synthesis of Pd Nanocrystals in Aqueous Solutions. *Adv. Funct. Mater.* **2009**, *19*, 189–200.
29. Mohanty, A.; Garg, N.; Jin, R. A Universal Approach to the Synthesis of Noble Metal Nanodendrites and Their Catalytic Properties. *Angew. Chem., Int. Ed.* **2010**, *49*, 4962–4966.
30. Sanchez-Gaytan, B. L.; Park, S.-J. Spiky Gold Nanoshells. *Langmuir* **2010**, *26*, 19170–19174.
31. Ellis, P. J.; Fairlamb, I. J. S.; Hackett, S. F. J.; Wilson, K.; Lee, A. F. Evidence for the Surface-Catalyzed Suzuki–Miyaura Reaction over Palladium Nanoparticles: An Operando XAS Study. *Angew. Chem., Int. Ed.* **2010**, *49*, 1820–1824.